Microbes and Infectious Diseases 2023; 4(3): 833-845

Microbes and Infectious Diseases

Journal homepage: https://mid.journals.ekb.eg/

Original article

Can gold nanoparticles enhance the antibacterial activity of vancomycin against methicillin-resistant *Staphylococcus aureus*?

Merna S. Abdelshakour [1], Abdullah M. Abdo [2], Nehad M. Sayed[1], Yasmin M. Ahmed [1*]

1- Medical Microbiology and Immunology Department, Faculty of Medicine, Ain Shams University, P.O. Box 1181, Abbassia, Cairo, Egypt.
2- Botany and Microbiology Department, Faculty of Science, Al-Azhar University, P.O. Box 11884, Nasr City, Cairo, Egypt.

ARTICLE INFO

Article history:
Received 21 June 2023
Received in revised form 11 July 2023
Accepted 15 July 2023

Keywords:
Methicillin-resistant.
Staphylococcus aureus.
Vancomycin.
Microwave.
Gold nanoparticles.
Vancomycin conjugated gold nanoparticles.

ABSTRACT

Background: Vancomycin is one of the main therapies for methicillin-resistant *S. aureus* (MRSA), however emergence of resistant strains is rising. Nanoparticles can offer promising solution. So, we studied the effect of gold nanoparticles (AuNPs) in enhancing vancomycin potential against MRSA clinical isolates from different types of infections. **Methods:** The susceptibility patterns of vancomycin, AuNPs, and vancomycin-conjugated gold nanoparticles (V-AuNPs) were evaluated on 30 MRSA isolates obtained from various clinical samples by using the microtiter broth dilution method. AuNPs and V-AuNPs were prepared by using a straightforward technique of microwave-assisted synthesis. **Results:** Twenty-seven (90%) MRSA isolates were susceptible to vancomycin and three (10%) showed intermediate susceptibility, with mean minimum inhibitory concentration (MIC) 2.68 ± 2.07 µg /ml, inhibitory concentration (conc.) to 50% of MRSA (IC50) 1.95 µg /ml and inhibitory conc. to 90% of the isolates (IC90) 3.9 µg /ml. While the synthesized AuNPs demonstrated a bactericidal effect on all the tested isolates with mean MIC 164.6 ± 62.5 µg /ml, IC50 125 µg /ml, and IC90 250 µg /ml. Meanwhile, V-AuNPs demonstrated synergistic bactericidal effect on all thirty (100%) tested MRSA isolates with mean MIC 0.40 ± 0.46 µg /ml, IC50 0.24 µg /ml, and IC 90 0.48 µg /ml. Moreover, V-AuNPs demonstrated minimal cytotoxic concentration up to 100 and 98.65 percent viability on human foreskin fibroblast (HFF-1) cell line at conc. of 2 µg/ml and 3.9 µg/ml respectively. **Conclusions:** The V-AuNPs display superior antibacterial activity as compared to vancomycin and AuNPs alone as a potentially effective therapy against MRSA.

Introduction

Methicillin-resistant *Staphylococcus aureus* (MRSA) is one of the most encountered resistant pathogens in clinical management. MRSA is transmitted in both healthcare and community settings and is associated with significant mortality, morbidity, and healthcare costs [1,2]. MRSA frequently causes serious infectious illnesses, such as pyogenic infections of the skin and soft tissues, suppurative pneumonia, otitis media, and pyogenic endocarditis [3].

Vancomycin is a potent glycopeptide antibiotic that is active against Gram-positive bacteria by interrupting cell wall synthesis [4]. In addition, vancomycin is still one of the main therapies for MRSA infections. However, *Staphylococcus aureus (S. aureus)* developed resistance to the antibiotic recently including vancomycin-intermediate *S. aureus* (VISA) and

DOI: 10.21608/MID.2023.219295.1549
* *Corresponding author: Yasmin M. Ahmed*
E-mail address: *dryasmin.mahmoud@med.asu.edu.eg*

vancomycin-resistant *Staphylococcus aureus* (VRSA)[5,6].

In addition to the development of bacterial resistance, vancomycin tissue penetration is highly variable and depends on the degree of inflammation. Specifically, penetration is limited for bone, lung epithelial lining fluid, and cerebrospinal fluid [7].

Nanotechnology offers an advanced discipline that has the potential to treat infections in novel ways using nanoparticles [8]. Nanoparticles can be used as antibacterial agents alone or in conjugation with antimicrobial agents [9].

Among noble nanomaterials, gold nanoparticles (AuNPs) have received a lot of concern due to their superior antibacterial action, inertness, non-toxicity, functionalization with biomolecules, ability to detect germs, and photothermal activity [10,11].

AuNPs can facilitate the delivery of relatively higher drug concentrations to the infection site while simultaneously minimizing drug toxicity. AuNPs are efficient in sustaining antibiotic release over a prolonged period, resulting in enhanced antibiotic efficacy [12]. This work aims to study the effect of AuNPs in enhancing vancomycin potential against MRSA clinical isolates from different types of infections.

Materials and methods

This study was approved by the Ethical Committee (FMASU MS 440/2022) of the Faculty of Medicine, Ain Shams University, Cairo.

This pilot study was conducted from July 2022 to October 2022 on thirty MRSA isolates obtained from inpatient and outpatient clinical samples submitted to the central microbiology laboratory at Ain Shams university hospital. The inclusion criteria were bacterial isolates that were confirmed to be methicillin-resistant *S.aureus* recovered from different types of infections and the exclusion criteria were bacterial isolates other than methicillin-resistant *S. aureus*.

Isolation and identification of MRSA

The collected isolates were subjected to conventional identification according to **Becker et al** [13]. Detection of methicillin resistance was done by cefoxitin (30µg) disk (Oxoid, England), using the disk diffusion method according to **Clinical and Laboratory Standards Institute guidelines (CLSI, 2022)** [14], *S. aureus* was considered MRSA when the zone of inhibition was ≤ 21mm as shown in **figure (1 b)**.

Synthesis and characterization of AuNPs and vancomycin-conjugated gold nanoparticles (V-AuNPs)** [15,16]

A straightforward, one-step method to synthesize AuNPs using microwave radiation was done by using gold precursor 5 ml of 1.27 mM (2.5 mg) of tetra chloroauric acid trihydrate ($HAuCl_4 \cdot 3H_2O$) (Loba Chimie, India), 39 mg of citric acid (Chem-Lab, Belgium) as a reducing agent, and 23.1 mg of acetyl trimethyl ammonium bromide (CTAB) (Loba Chimie, India) as a binding agent, they were mixed in an Erlenmeyer flask to get an aqueous solution. This solution was stirred for 15 seconds and then heated in a microwave oven (LG electronics, China; 1000 W) for 90 seconds to generate AuNPs, and a slight change in the color of the solution was observed then V-AuNPs was generated by adding 5 ml of 0.5 mg vancomycin to 5 ml of the previously prepared reaction mixture, stirring for 15 seconds, and then heating it in the microwave oven for 90 seconds. The color change was observed indicating the completion of the reaction.

AuNPs and V-AuNPs were characterized by visual observation of color change, uv- visible (UV-Vis) spectroscopy was done at a range of 400–800 nm (Cary series UV-Vis- NIR, Australia). Also, high-resolution transmission electron microscopy (HRTEM) (JEOL JEM-2100 high-resolution transmission electron microscope) equipped with Gatan digital camera Erlangshen ES500 was used to assess the homogeneity, morphology, and size of AuNPs and V-AuNPs nanoparticles. A dynamic light scattering zeta potential analyzer (Panalytical Zeta sizer nano-ZS, Malvern Ltd., UK) was used to measure the average particle size, charge density, and dynamic light scattering (DLS) present on the outer surface of the produced AuNPs and V-AuNPs. To examine the phase and crystalline structure of the synthesized AuNPs and V-AuNPs, an X-ray diffractometer (Panalytical X'Pert Pro, Netherlands) was used, and the results were compared to the widely used Joint Committee on Powder Diffraction Standards (JCPDS) library of AuNPs. In addition, fourier transform infrared (FTIR) spectra obtained from the purified nanoparticles were used to find out the possible molecules associated with the reduction of Au+ ions and capping and stabilizing of synthesized AuNPs. Also, to evaluate the

conformational changes upon the loading of vancomycin onto the external surface of AuNPs. The KBr pellet method was implemented to acquire FTIR spectra with (an FT-IR vertex 70 RAM II, Bruker Spectrometer). The functional groups contained in the sample were identified by comparing the obtained spectral data to the references.

MRSA susceptibility test using microtiter broth dilution method [16,17, 18]

In vitro, the MRSA susceptibility test was done by the microtiter broth dilution method. The tested substances were adjusted at double-fold dilution in nutrient broth, the concentration of vancomycin ranged from 125 µg/ml to 0.24 µg/ml, gold nanoparticles from 500 µg/ml to 0.97 µg/ml, and vancomycin conjugated gold nanoparticles from 7.8 µg/ml to 0.015 µg/ml.

Each well of the microtitre plate contained 100 µl of each previously prepared concentration, then 10 µl of the bacterial suspension was added into each well. This suspension was adjusted to 0.5 McFarland standard. Then further dilution at 1:20 was done to reach 5×10^6 CFU/ml.

Positive control wells included the organism in addition to broth, while negative control wells included the tested antibacterial substance in broth. The microtiter plates were then incubated at 37°C for 24 hours.

After overnight incubation, a resazurin microtiter plate assay was used to determine the minimum inhibitory concentration (MIC) of vancomycin alone, AuNPs, and V-AuNPs for each isolate, where resazurin dye (Sigma-Aldrich, Germany) changed color from blue to pink if viable cells are present. After incubating the overnight cultures with 0.015% resazurin for 4 hours, the MIC was determined as the concentration at which there was no color change [19]. The interpretation of MIC susceptibility breakpoints to vancomycin was determined according to CLSI standards [14].

Cytotoxicity evaluation [20,21]

Human foreskin fibroblast cells (HFF-1) were seeded in a 96-well plate at a cell density of 1×10^4 cells per well in 100 µl of growth media (Roswell park memorial institute (RPMI 1640) containing 10% fetal bovine serum, 2 mM L-glutamine and 1µg/ml gentamycin). After 24 hours, serial two-fold dilutions of V-AuNPs were added to confluent cell monolayers in the wells. The microtiter plates were incubated at 37 °C in a humidified incubator with 5% CO_2 for 24 hours. 3-(4,5-dimethylthiazol-2-yl)-2,5-diphenyltetrazolium bromide (MTT) test was done to determine the number of viable cells after a 24-hour incubation period, then plates were additionally incubated for 4 hours at 37°C with 5% CO_2. An 85 µl aliquot of the media was removed and 50 µl of Dimethyl sulfoxide (DMSO) was added then incubated at 37 °C for 10 minutes. The number of living cells was then determined by measuring the optical density at 590 nm using a microplate reader (Sunrise, TECAN, Inc., USA), and the viability percentage was computed as follows:

$$[(ODt/ODc)]x100\%$$

ODc referred to the mean optical density of untreated cells and ODt referred to the mean optical density of wells treated with the test material. The relationship between viable cells and drug concentration was plotted using GraphPad Prism Software (San Diego, CA. USA). The cytotoxic concentration (CC50), or the concentration needed to cause toxicity in 50% of intact cells, was calculated. Also, microscopic observation of HFF-1 cells treated with V-AuNPs was done, After the termination of the cytotoxicity assay procedure, plates were washed three times with phosphate-buffered saline, fixed with 10% formalin, stained with crystal violet, rinsed with deionized water, and dried. Then, using an inverted microscope (CKX41; Olympus, Japan) provided with a digital microscopy camera, the cellular morphology was compared to control cells.

Statistical analysis

Data were analyzed using the Statistical Package for Social Sciences (SPSS version 27). Descriptive analyses were performed to obtain the mean, standard deviation (SD), median, and interquartile range (IQR) for quantitative data, and Numbers and frequencies for qualitative data. Scatter graphs were used to show the correlations between different quantitative variables. Bivariate analyses were performed using the Chi-square test, Pearson correlation, and Kruskal-Wallis test. P value < 0.05 was regarded as significant.

Results

Synthesis of AuNPs and V-AuNPs and their Characterization

AuNPs synthesis was preliminarily confirmed within 3 minutes by a characteristic color change from the shining yellow color of the solution

of $HAuCl_4 \cdot 3H_2O$ into shining burgundy red color indicating the formation of AuNPs, while the color change from the shining burgundy red color of the AuNPs into faint purple color indicated the formation of V-AuNPs. Moreover, The Synthesis of AuNPs and V-AuNPs was confirmed by UV-vis spectra that showed sharp absorption peaks at 520 and 550 nm characteristic for AuNPs and V-AuNPs respectively. By using HRTEM, AuNPs were spherical and irregular in shape, with an average size of 3: 15 nm, and a mean diameter of 9±0.7 nm. Concerning V-AuNPs, characteristic star-shaped particles were detected in addition to the formally mentioned shapes, with an average size of 3:39 nm, and a mean diameter of 20.25± 1.07 nm viewed at (100000x). These sizes for AuNPs and V-AuNPs are suitable for use as antibacterial materials. In Zeta potential measurements, AuNPs and V-AuNPs had an average surface charge of −4.68 ± 3.17 mV and −5.75 ± 6.17 mV at pH *5* and an average size of 101.2±0.3 nm and 106.3± 0.45 nm, respectively, these values indicated stable nanoparticles and less liability to aggregate with time. The XRD pattern of AuNPs and V-AuNPs showed five diffraction peaks indexed to the (111), (200), (220), (311) and (222) reflections of the face-centered cubic structure of metallic gold (JCPDS No. 04-0784). FTIR spectra showed ranged intense peaks at 3284.59 cm^{-1} for AuNPs and 3276.71 cm^{-1} for V-AuNPs, indicating the existence of the O-H functional group and H bond of alcoholic and phenolic compounds. the absorption at 1638.09, 1045.36 cm^{-1} for AuNPs, and 1636.25 cm^{-1} for V-AuNPs corresponded to C═C stretching vibrations of an aromatic alkene and N-H functional groups of primary and secondary amines of amino acids and peptides. While the peaks at 558.47, 501.98, 454.91, 425.87 cm^{-1} for AuNPs and 550.29, 488.93, 438.42, and 419.47 cm^{-1} for V-AuNPs were attributed to out-of-plane C–H bending vibrations in alkenes and aromatics, these results indicate the presence of vancomycin in V-AuNPs establishing the efficient loading vancomycin onto the surface of AuNPs, as shown in **fig (2a-e)**.

Sources of MRSA isolates

Thirty MRSA isolates were collected from different clinical samples mainly from blood (11/30, 37%), then wound swabs (8/30, 27%), sputum (5/30, 17%), pus (3/30, 10%), pleural fluid (1/30, 3%), bronchial lavage (1/30, 3%), and urine (1/30, 3%) as shown in **figure (3)**.

Susceptibility of MRSA isolates to vancomycin, AuNPs, and V-AuNPs

the MRSA susceptibility test was done by the microtiter broth dilution method as shown in **fig (4)**. Twenty-seven (90%) MRSA isolates were susceptible to vancomycin and 3 (10%) showed intermediate susceptibility. Thirty (100%) MRSA isolates were susceptible to AuNPs and V-AuNPs as shown in **table (1a).**

The values of mean MIC of vancomycin, AuNPs, and V-AuNPs are mentioned in **table (1b)**. It is worth noting that the 3 (10%) intermediate-susceptible isolates to vancomycin were converted to be sensitive to V-AuNPs at much lower doses to vancomycin, where intermediate-susceptible isolates to vancomycin showed mean MIC ± SD as 6.24 ± 2.14 µg /ml for vancomycin alone, while showed mean MIC ± SD as 1.17 ± 0.74 µg /ml for V-AuNPs.

The MIC values of vancomycin were directly proportional to the MIC values of V-AuNPs with statistically significant differences, as shown in **figure (5)**.

Cytotoxicity evaluation

Based on cell viability by MTT assay, the in-vitro cytotoxic effects of the synthesized V-AuNPs were assessed against the HFF-1 cell line. HFF-1 cells treated with V-AuNPs at concentrations of 2, and 3.9 µg/ml showed 100% and 98.65% viability after the incubation period, respectively; the viability of HFF-1 cells decreased with increasing V-AuNPs concentration gradually. At the same time, viability dropped to almost 50% of the initial level, which showed 50%, at a concentration of 33.85± 3.16 µg/ml. So, these values were selected as the CC50 concentration. Also, the lowest viability percentages of 4.72% and 0.98%, respectively, were reported at maximal concentrations of 250 and 500 µg/ml, as illustrated in **figure (6 A-D)**.

Figure 1. Conventional identification of methicillin-resistant *Staphylococcus aureus* (MRSA).

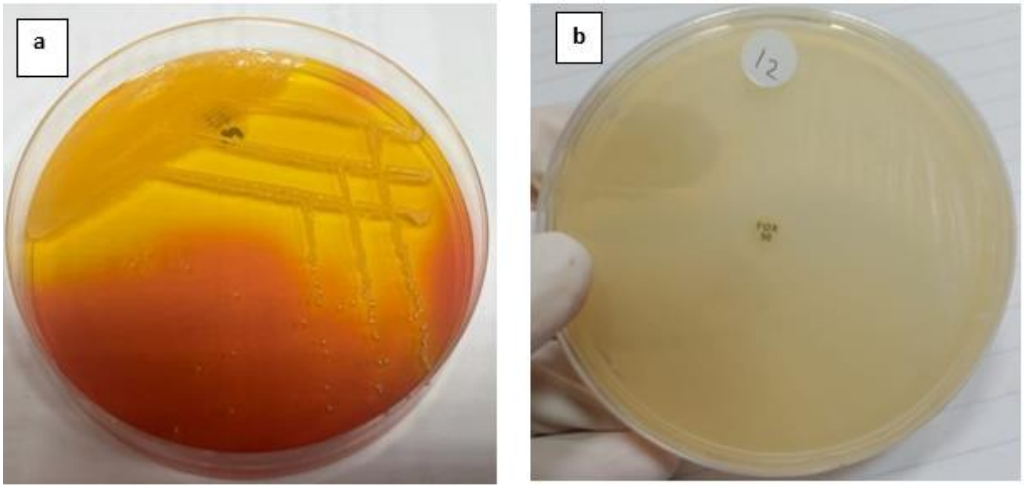

(a): Yellow colonies of *S. aureus* on mannitol salt agar.
(b): Mueller-Hinton agar plate with cefoxitin disc diffusion method showing methicillin-resistant *S. aureus* (with no inhibition zone)**.**

Figure 2. Microwave-assisted synthesis and characterization of AuNPs and V-AuNPs.

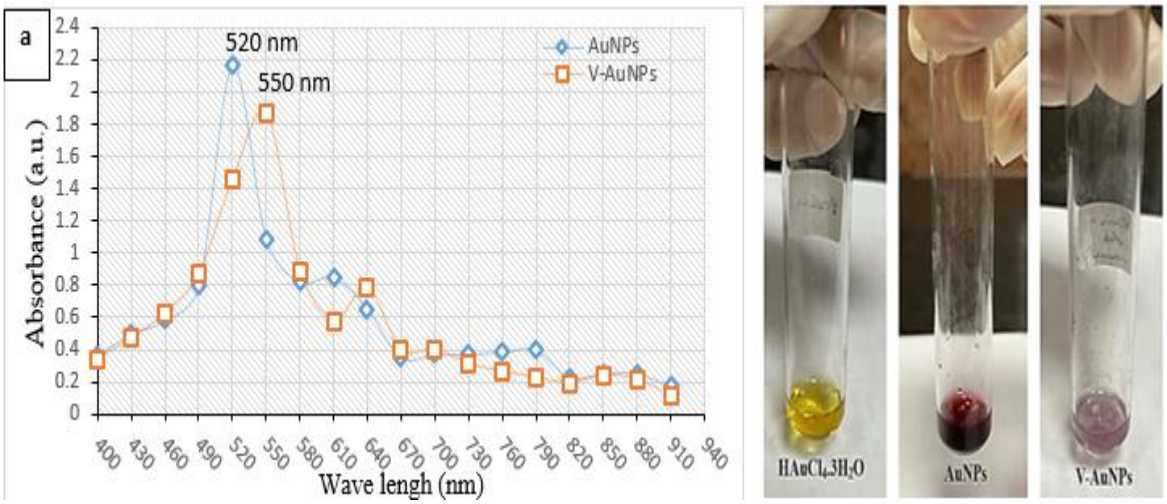

(a): Visible observation and UV-visible spectroscopy AuNPs and V-AuNPs.

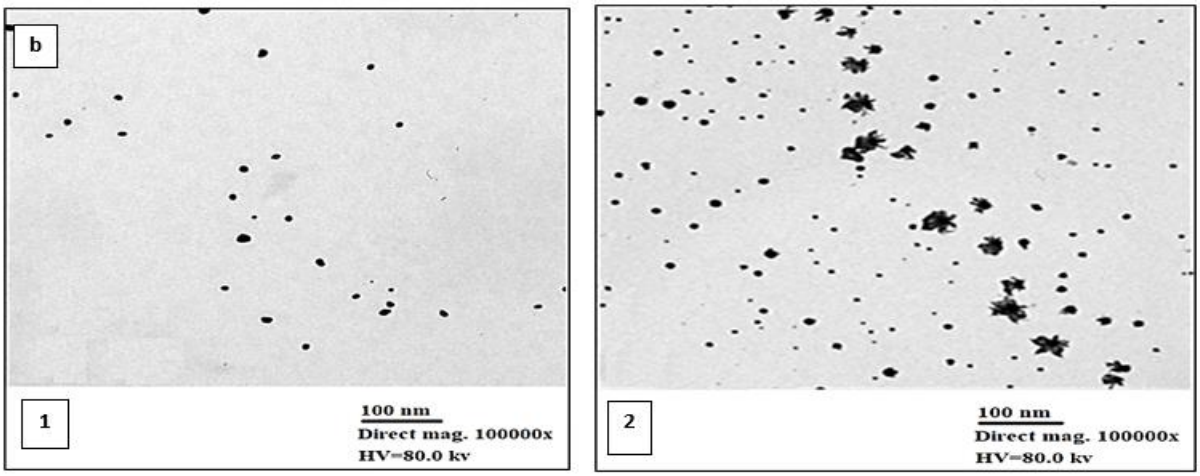

(b): HRTEM of microwave-assisted synthesis of AuNPs (1) and V-AuNPs (2).

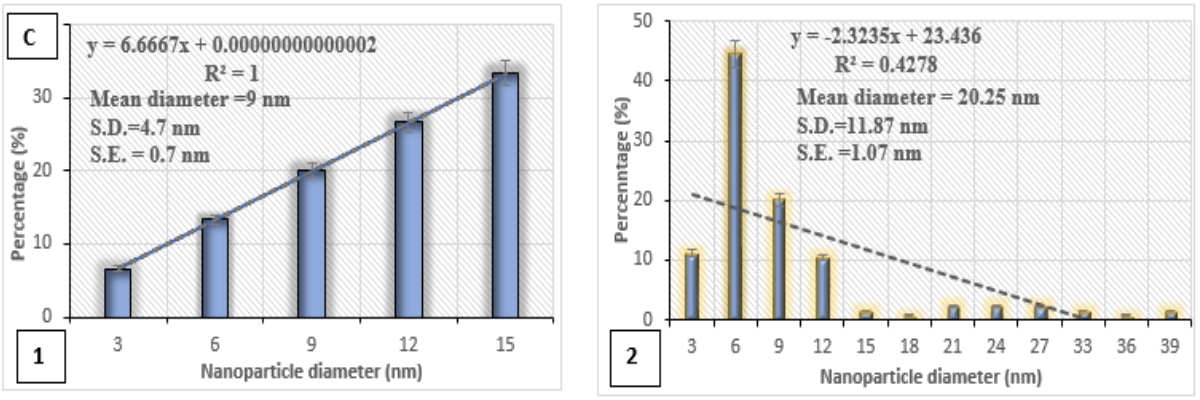

(c): Particle size distribution by HRTEM image of AuNPs (1) and V-AuNPs (2).

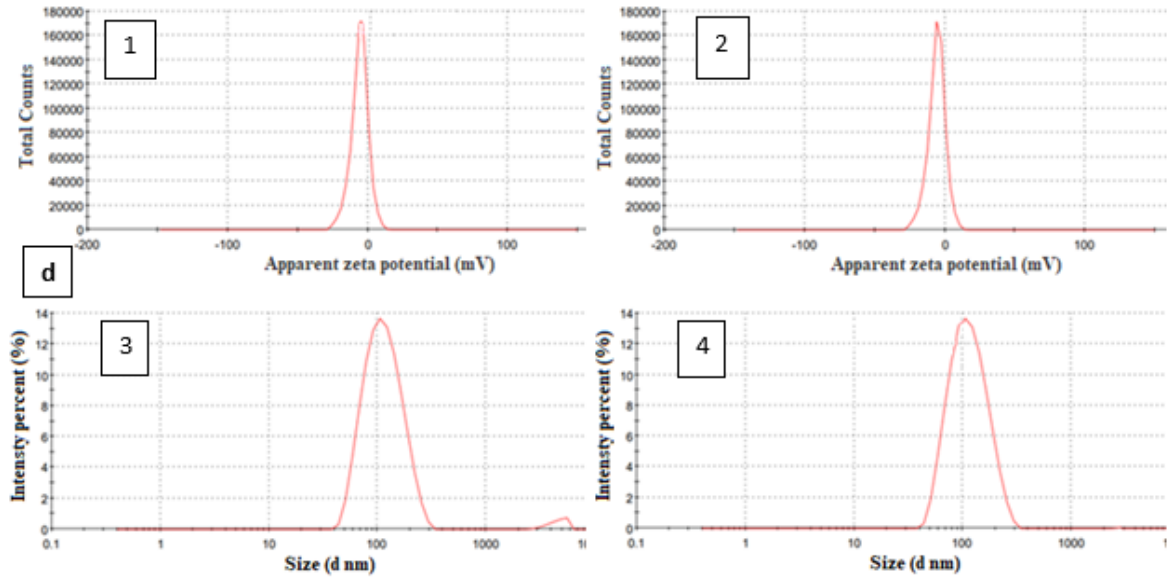

(d): 1, 3 Zeta Potential and DLS of AuNPs and 2, 4 Zeta Potential and DLS of V-AuNPs.

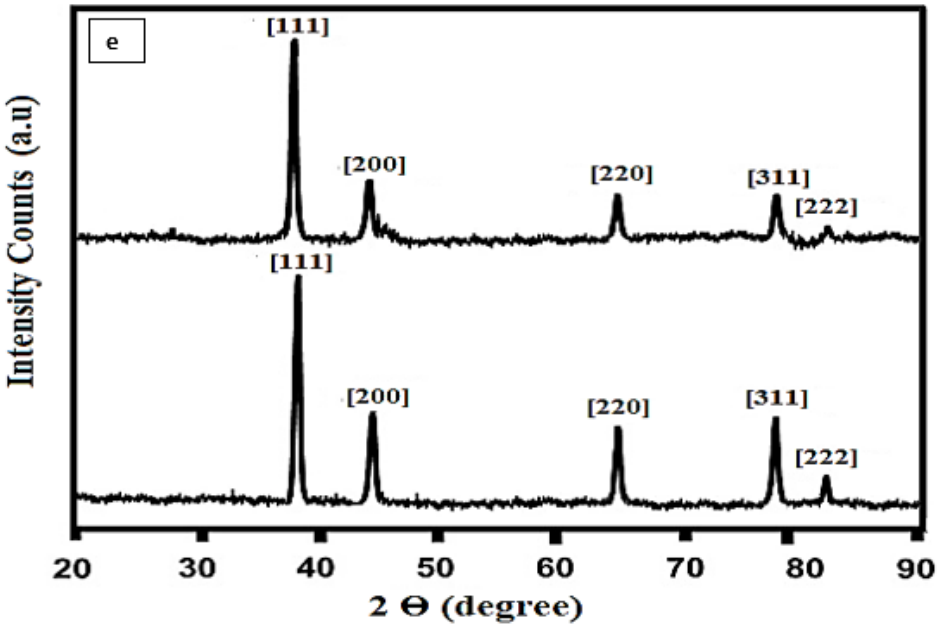

(e): XDR patterns of (1) AuNPs and (2) V-AuNPs.

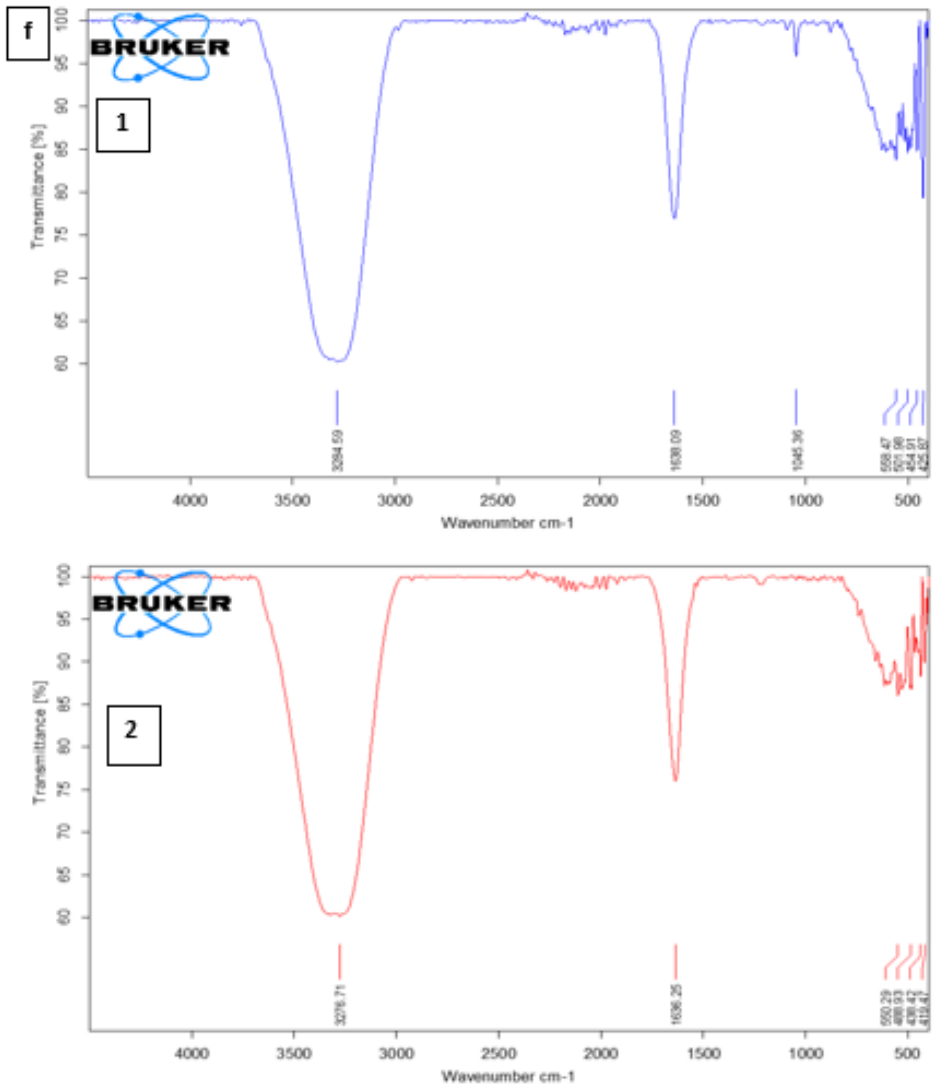

(f): FTIR measurements of (A) AuNPs and (B) V-AuNPs.

Figure 3. Pie chart showing proportions of different MRSA clinical samples.

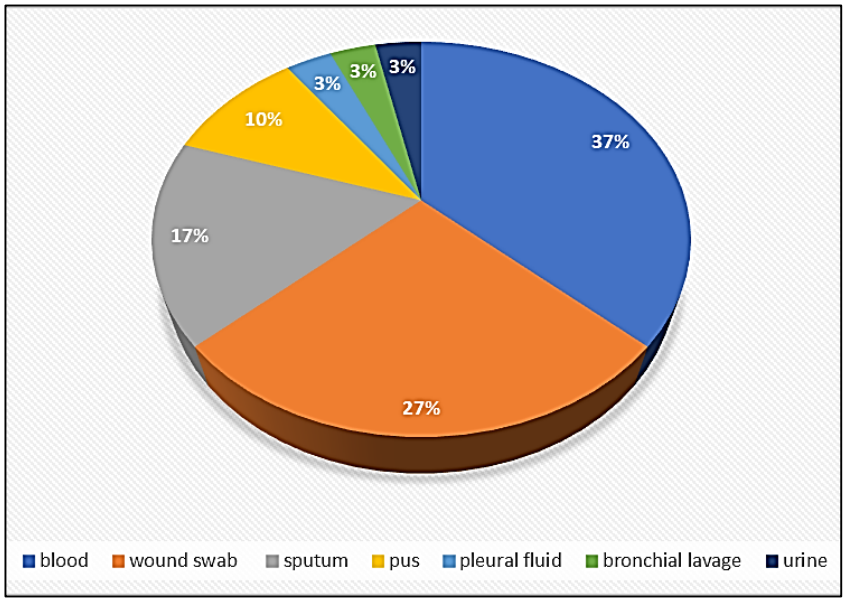

Figure 4. MIC determination of vancomycin, AuNPs, and V-AuNPs against MRSA isolates.

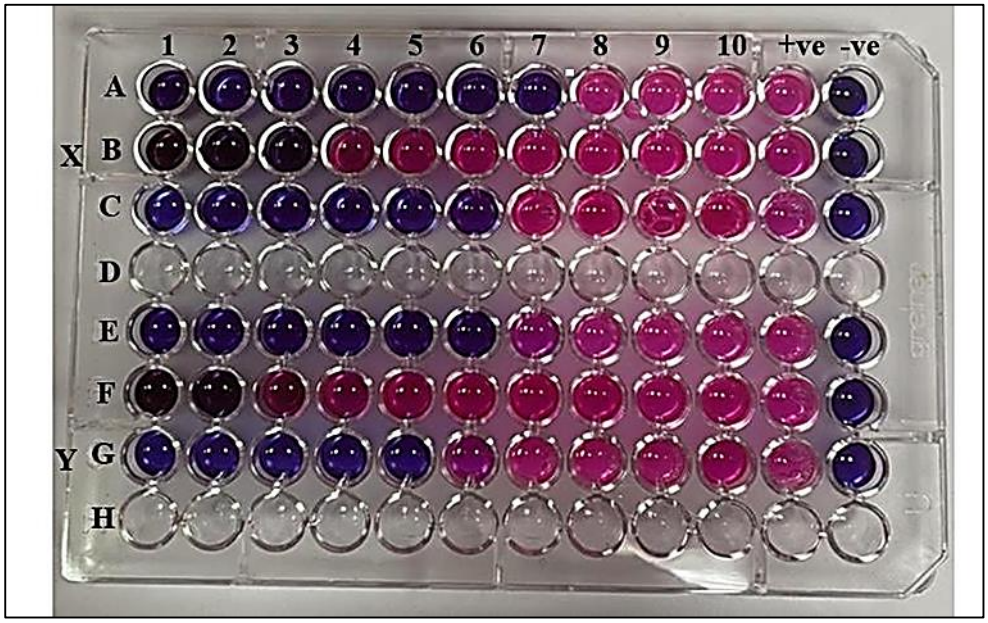

Rows (A, B, C, E, F, and G) represent the testing of vancomycin, AuNPs, and V-AuNPs respectively against isolates (X and Y). For sample (X), in row (A) column (7) represents the MIC of vancomycin (1.95 µg/ml), in row (B) column (3) represents the MIC of AuNPs (125 µg/ml), and in row (C), column (6) represents MIC of V-AuNPs (0.24 µg/ml). +ve and –ve controls were added in as shown.

Table 1a. Determination of MIC ranges of the used antibacterial agents against MRSA isolates according to microtiter broth dilution technique.

Antibacterial agent	MIC (µg /ml)				Number and (%) of susceptibility patterns among the diff. isolates	
	Range	Mean± SD	IC 50	IC 90	Susceptible isolates	Intermediate isolates
Vancomycin	0.48-7.8	2.68± 2.07	1.95	3.9	27 (90%)	3 (10%)
AuNPs	125-250	164.6 ± 62.5	125	250	30 (100%)	0 (0%)
V-AuNPs	0.06-1.95	0.40 ± 0.46	0.24	0.48	30 (100%)	0 (0%)

IC 50: Inhibitory concentration for 50% of the isolated MRSA.
IC 90: Inhibitory concentration for 90% of the isolated MRSA.
N.B. The isolates that have MIC range between 2.1 and 3.9 µg /ml were counted as vancomycin susceptible.

Table 1b. The values of mean MIC of vancomycin, AuNPs, and V-AuNPs.

Number of MRSA isolates	Variables			P value
	Vancomycin mean MIC ± SD (µg /ml)	AuNPs mean MIC ± SD (µg /ml)	V-AuNPs mean MIC ± SD (µg /ml)	
30	2.68 ± 2.07	164.6 ± 62.5	0.40 ± 0.46	<0.001*

Figure 5. MIC Correlation of vancomycin and V-AuNPs.

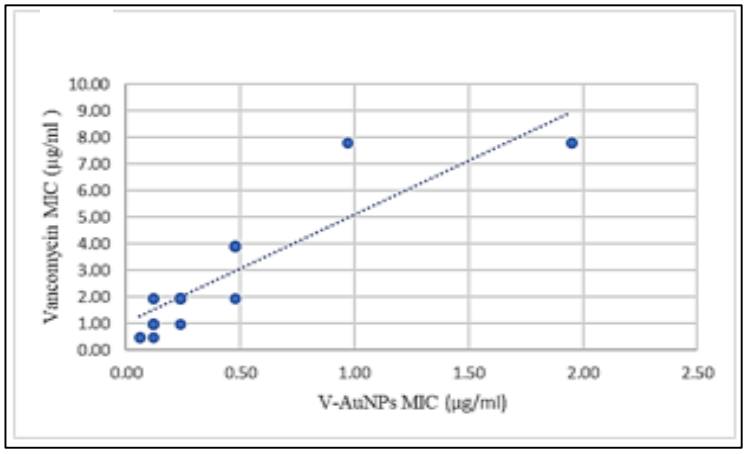

(r = 0.91, P value<0.001*).

Figure 6. Cytotoxicity and morphological evaluation by MTT assay of V-AuNPs treated HFF-1 cells, at different concentrations and overnight incubation.

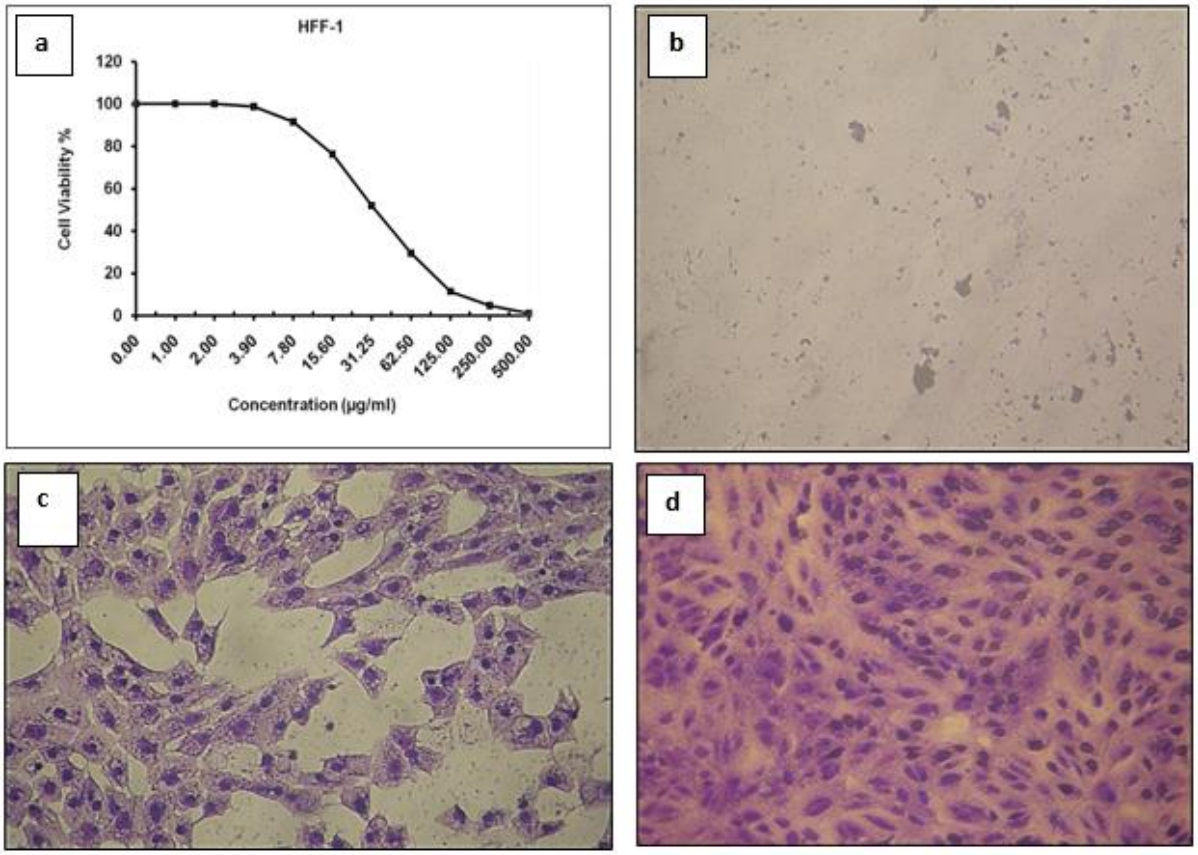

(a): Cytotoxicity by MTT assay of V-AuNPs against HFF-1 cell line.
(b): HFF-1 cells treated with V-AuNPs at 500 µg/ml concentration.
(c): HFF-1 cells treated with V-AuNPs At 50 µg/ml concentration.
(d): HFF-1 cells non-treated (control).

Discussion

One of the biggest global issues affecting people's health today is MRSA. It is widely spread and can cause high rates of mortality and medical expenses. [22]. In the current study, MRSA isolates were collected mainly from blood and wound swabs, with 37% and 27%, respectively. Vancomycin was a dependable therapy for treating MRSA infections.

Concerningly, there have been reports of vancomycin susceptibility declining [23]. In the current study, twenty-seven MRSA isolates (90%) were susceptible to vancomycin and 3 isolates (10%) showed intermediate susceptibility. MIC ranged from 0.48 to 7.8 µg /ml, mean MIC was 2.68 µg /ml, (IC50) was 1.95 µg /ml, and (IC90) was 3.9 µg /ml.

These results came in agreement with **Elfeky et al.** [24] who found that 85% of MRSA isolates were susceptible to vancomycin and 15% were intermediately susceptible to vancomycin. Another study done by **There et al.** [25] showed that 86.85% of isolates were sensitive to vancomycin and 13.15% were resistant to vancomycin. Additionally, vancomycin had a MIC range of 0.5 to 8 µg/ml, IC50 was 2 µg/ml and IC90 was 4 µg/ml according to **Periasamy et al.** [26].

Moreover, **Dandan et al.** [27] reported that all MRSA isolates were sensitive to vancomycin with IC 50 0.5 µg/ml and IC 90 1 µg/ml. **Augusto et al.** [28] showed susceptibility of all MRSA isolates to vancomycin where both IC 50 and IC 90 were 2 µg/ml, and the MIC range was 0.5-2 µg/ml. These results showed different values of MIC and different values of IC 50 and IC 90. This may be attributed to obtaining isolates from different samples, different geographical areas, or measuring MIC by a different technique.

AuNPs have displayed uniquely advantageous antimicrobial activity through their effect on apoptosis, cell membrane damage, DNA damage, reactive oxygen species creation, and disruption of metabolic pathways. [11].

In this study, thirty MRSA isolates were sensitive to AuNPs with MIC ranging from 125 to 250 µg /ml, with mean MIC ± SD 164.6 ± 62.5 µg /ml, with IC50 125 µg /ml and IC90 250 µg /ml.

Similar results were obtained by **Muthukumar et al.** [29], where the green synthesized AuNPs using leaf extracts of Carica papaya had an antibacterial effect against *S. aureus* with MIC 125 µg /ml. **Murei et al.** [30] assessed the sensitivity of chemically synthesized gold nanoparticles by two methods. The disk diffusion method showed the high effectiveness of these NPs against MRSA with a zone of inhibition of 27 mm. and the microtiter broth dilution method was also effective against MRSA with MIC 100 µg /ml.

Studies have shown that conjugating antibiotics with AuNPs can improve their antibacterial effectiveness while minimizing side effects by lowering the need for high antibiotic doses [16,31].

As regards the V-AuNPs, the MIC range was 0.06 to 1.95 µg /ml, mean MIC ± SD was 0.40 ± 0.46 µg /ml, IC50 was 0.24 µg /ml and IC 90 was 0.48 µg /ml, these results are much lower than those of vancomycin alone, revealing that V-AuNPs has better antibacterial effect than vancomycin alone.

In Taiwan, **Lai et al.** [32] agreed with the results of the current study where IC 50 of vancomycin alone against MRSA was 64 µg /ml while IC 50 of V-AuNPs was 8 µg /ml, showing a better antibacterial effect for V-AuNPs than vancomycin alone. A difference that is highly statistically significant was found between the IC 50 values of vancomycin and V-AuNPs and between AuNPs and V-AuNPs and this agreed with **Hagbani et al.** [16] who found that the IC 50 of vancomycin alone against *S. aureus* was 48.18 µg /ml, while IC 50 of V-AuNPs was 30.63 µg /ml, revealing the promising antibacterial effect of V-AuNPs that was much more effective at lower doses than vancomycin alone against *S. aureus*.

Concerning cytotoxicity of V-AuNPs to HFF-1 cells, using a concentration of 2 µg/ml of V-AuNPs gave 100% viability of the cells, while raising the concentration to 33.85± 3.16 µg/ml, viability was dropped to 50% and raising the conc. to 250 µg/ml, viability was dropped to 4.72%, indicating that the used conc. range in this study was safe for the HFF-1 cells.

Steckiewicz et al. [33] stated that V-AuNPs' antiproliferative efficacy is influenced by both size and shape and V-AuNPs' shape-dependent characteristics make them suitable for therapeutic use. In a similar vein, **Mahmoud et al.** [34] found that the surface coatings of gold nanorods had a significant impact on their ability to penetrate human dermal fibroblasts and maintain cellular viability with minimal cytotoxicity.

The findings in this study indicate that V-AuNPs display superior antibacterial activity as compared to vancomycin and AuNPs alone as a potentially effective therapy against MRSA.

Competing nterests
Non declared.

Funding
Non declared.

References

1. **Tigabu A, Getaneh A.** *Staphylococcus aureus*, ESKAPE Bacteria Challenging Current Health Care and Community Settings: a Literature Review. *Clin Lab*. 2021;67(7):10-7754. doi:10.7754/Clin.Lab.2020.200930.
2. **Garoy EY, Gebreab YB, Achila OO, Tekeste DG, Kesete R, Ghirmay R, et al.** Methicillin-Resistant *Staphylococcus aureus* (MRSA): Prevalence and Antimicrobial Sensitivity Pattern among Patients—A Multicenter Study in Asmara, Eritrea. *Canadian Journal of Infectious Diseases and Medical Microbiology*. 2019;2019:1-9. doi:10.1155/2019/8321834.
3. **Algammal AM, Hetta HF, Elkelish A, Alkhalifah DH, Hozzein WN, Batiha GE, et al.** Methicillin-Resistant *Staphylococcus aureus* (MRSA): one health perspective approach to the bacterium epidemiology, virulence factors, antibiotic-resistance, and zoonotic impact. *Infection and Drug Resistance*. 2020; 13:3255-3265.
4. **Sarkar P, De K, Modi M, Dhanda G, Priyadarshini R, Bandow JE, et al.** Next-generation membrane-active glycopeptide antibiotics also inhibit bacterial cell division. *Chem Sci*. 2023;14(9):2386-2398. doi:10.1039/D2SC05600C.
5. **Haas K, Meyer-Buehn M, von Both U, Hübner J, Schober T.** Decrease in vancomycin MICs and prevalence of hGISA in MRSA and MSSA isolates from a German pediatric tertiary care center. *Infection*. Published online April 18, 2023. doi:10.1007/s15010-023-02036-5.
6. **Guo Y, Song G, Sun M, Wang J, Wang Y.** Prevalence and Therapies of Antibiotic-Resistance in *Staphylococcus aureus*. *Front Cell Infect Microbiol*. 2020;10. doi:10.3389/fcimb.2020.00107.
7. **Jager NGL, van Hest RM, Lipman J, Roberts JA, Cotta MO.** Antibiotic exposure at the site of infection: principles and assessment of tissue penetration. *Expert Rev Clin Pharmacol*. 2019;12(7):623-634. doi:10.1080/17512433.2019.1621161.
8. **Haleem A, Javaid M, Singh RP, Rab S, Suman R.** Applications of nanotechnology in the medical field: a brief review. *Global Health Journal*. Published online February 2023. doi:10.1016/j.glohj.2023.02.008.
9. **Sánchez-López E, Gomes D, Esteruelas G, Bonilla L, Lopez-Machado AL, Galindo R, et al.** Metal-Based Nanoparticles as Antimicrobial Agents: An Overview. *Nanomaterials*. 2020;10(2):292. doi:10.3390/nano10020292.
10. **Naskar A, Kim K sun.** Nanomaterials as Delivery Vehicles and Components of New Strategies to Combat Bacterial Infections: Advantages and Limitations. *Microorganisms*. 2019;7(9):356. doi:10.3390/microorganisms7090356.
11. **Mobed A, Hasanzadeh M, Seidi F.** Anti-bacterial activity of gold nanocomposites as a new nanomaterial weapon to combat photogenic agents: recent advances and challenges. *RSC Adv*. 2021;11(55):34688-34698. doi:10.1039/D1RA06030A.
12. **Sibuyi NRS, Moabelo KL, Fadaka AO, Meyer S, Onani MO, Madiehe AM, et al.**

Multifunctional Gold Nanoparticles for Improved Diagnostic and Therapeutic Applications: A Review. *Nanoscale Res Lett*. 2021;16(1):174. doi:10.1186/s11671-021-03632-w.

13. **Becker K, Skov RL, von Eiff C.** *Staphylococcus* , *Micrococcus* , and Other Catalase-Positive Cocci. In: *Manual of Clinical Microbiology*. ASM Press; 2015:354-382. doi:10.1128/9781555817381.ch21.
14. **CLSI.** Performance Standards for Antimicrobial Susceptibility Testing A CLSI supplement for global application, 32nd Edition M100 .Wayne, PA: Clinical and Laboratory Standards Institute; 2022; [Online]. Available: www.clsi.org.
15. **Gutiérrez-Wing C, Esparza R, Vargas-Hernández C, Fernández García ME, José-Yacamán M.** Microwave-assisted synthesis of gold nanoparticles self-assembled into self-supported superstructures. *Nanoscale*. 2012;4(7):2281. doi:10.1039/c2nr12053d.
16. **Hagbani T Al, Yadav H, Moin A, Lila ASA, Mehmood K, Alshammari F, et al.** Enhancement of Vancomycin Potential against Pathogenic Bacterial Strains via Gold Nano-Formulations: A Nano-Antibiotic Approach. *Materials*. 2022;15(3):1108. doi:10.3390/ma15031108.
17. **Hashim MH.** The synergistic effect of biosynthesized gold nanoparticles with antibiotic against clinical isolates. *Journal of Biotechnology Research Center*. 2019;13(1):58-62.
18. **CLSI.** Methods for dilution antimicrobial susceptibility tests for bacteria that grow aerobically, 11th edition Approved standard M07-A11. Wayne, PA: Clinical and Laboratory Standards Institute; 2018.
19. **Chakansin C, Yostaworakul J, Warin C, Kulthong K, Boonrungsiman S.** Resazurin rapid screening for antibacterial activities of organic and inorganic nanoparticles: Potential, limitations and precautions. *Anal Biochem*. 2022;637:114449. doi:10.1016/j.ab.2021.114449.
20. **Bahuguna A, Khan I, Bajpai VK, Kang SC.** MTT assay to evaluate the cytotoxic potential of a drug. *Bangladesh J Pharmacol*. 2017;12(2). doi:10.3329/bjp.v12i2.30892.
21. **Abo-Ashour MF, Eldehna WM, Nocentini A, Bonardi A, Bua S, Ibrahim HS, et al.** 3-Hydrazinoisatin-based benzenesulfonamides as novel carbonic anhydrase inhibitors endowed with anticancer activity: Synthesis, in vitro biological evaluation and in silico insights. *Eur J Med Chem*. 2019;184:111768. doi:10.1016/j.ejmech.2019.111768.
22. **Liu F, Rajabi S, Shi C, Afifirad G, Omidi N, Kouhsari E, et al.** Antibacterial activity of recently approved antibiotics against methicillin-resistant *Staphylococcus aureus* (MRSA) strains: A systematic review and meta-analysis. *Ann Clin Microbiol Antimicrob*. 2022;21(1):37. doi:10.1186/s12941-022-00529-z.
23. **Du M, Song L, Wang Y, Suo J, Bai Y, Xing Y,et al.** Investigation and control of an outbreak of urinary tract infections caused by Burkholderia cepacian-contaminated anesthetic gel. *Antimicrob Resist Infect Control*. 2021;10(1):1. doi:10.1186/s13756-020-00855-x.

24. **ElFeky DS, Awad AR, Elshobaky MA, Elawady BA.** Effect of ceftaroline, vancomycin, gentamicin, macrolides, and ciprofloxacin against methicillin-resistant *Staphylococcus aureus* isolates: An in vitro study. *Surgical Infections*. 2020;21(2):150-7.
25. **There YW, Wadhai VS, Bhandari P.** Prevalence of vancomycin resistance *Staphylococcus aureus* among MRSA isolates from district hospital Gadchiroli (ms) India. *IJRBAT*. 2018;4(1):214-8.
26. **Periasamy H, Iswarya S, Pavithra N, Senthilnathan S, Gnanamani A.** *In vitro* antibacterial activity of plumbagin isolated from *Plumbago zeylanica* L. against methicillin-resistant *Staphylococcus aureus*. *Lett Appl Microbiol*. Published online May 2, 2019:lam.13160. doi:10.1111/lam.13160.
27. **Dandan Y, Shi W, Yang Y, Yonggui Z, Zhu D, Yan G, et al.** Antimicrobial activity of ceftobiprole and comparator agents when tested against gram-positive and -negative organisms collected across China (2016–2018). *BMC Microbiol*. 2022;22(1):282. doi:10.1186/s12866-022-02699-4.
28. **Augusto MF, da Silva Fernandes DC, de Oliveira TLR, Cavalcante FS, Chamon RC, Ferreira ALP, et al.** Pandemic clone USA300 in a Brazilian hospital: detection of an emergent lineage among methicillin-resistant *Staphylococcus aureus* isolates from bloodstream infections. *Antimicrob Resist Infect Control*. 2022;11(1):114. doi:10.1186/s13756-022-01154-3.
29. **Muthukumar T, Sudhakumari, Sambandam B, Aravinthan A, Sastry TP, Kim JH.** Green synthesis of gold nanoparticles and their enhanced synergistic antitumor activity using HepG2 and MCF7 cells and its antibacterial effects. *Process Biochemistry*. 2016;51(3):384-391. doi:10.1016/j.procbio.2015.12.017.
30. **Murei A, Pillay K, Samie A.** Syntheses, Characterization, and Antibacterial Evaluation of P. grandiflora Extracts Conjugated with Gold Nanoparticles. *J Nanotechnol*. 2021;2021:1-10. doi:10.1155/2021/8687627.
31. **Fuller M, Whiley H, Köper I.** Antibiotic delivery using gold nanoparticles. *SN Applied Sciences.* 2020; 2:1-7.
32. **Lai HZ, Chen WY, Wu CY, Chen YC.** Potent Antibacterial Nanoparticles for Pathogenic Bacteria. *ACS Appl Mater Interfaces*. 2015;7(3):2046-2054. doi:10.1021/am507919m.
33. **Steckiewicz KP, Barcinska E, Malankowska A, Zauszkiewicz–Pawlak A, Nowaczyk G, Zaleska-Medynska A, et al.** Impact of gold nanoparticles shape on their cytotoxicity against human osteoblast and osteosarcoma in in vitro model. Evaluation of the safety of use and anti-cancer potential. *J Mater Sci Mater Med*. 2019;30(2):22. doi:10.1007/s10856-019-6221-2.
34. **Mahmoud NN, Al-Kharabsheh LM, Khalil EA, Abu-Dahab R.** Interaction of Gold Nanorods with Human Dermal Fibroblasts: Cytotoxicity, Cellular Uptake, and Wound Healing. *Nanomaterials*. 2019;9(8):1131. doi:10.3390/nano9081131.